

Ultrathin Films of Ferroelectric Solid Solutions under a Residual Depolarizing Field

Igor Kornev, Huaxiang Fu, and L. Bellaiche

Physics Department, University of Arkansas, Fayetteville, Arkansas 72701, USA

(Received 17 March 2004; published 5 November 2004)

A first-principles-derived approach is developed to study the effects of depolarizing electric fields on the properties of $\text{Pb}(\text{Zr}, \text{Ti})\text{O}_3$ ultrathin films for different mechanical boundary conditions. A rich variety of ferroelectric phases and polarization patterns is found, depending on the interplay between strain and the amount of screening of surface charges. Examples include triclinic phases, monoclinic states with in-plane and/or out-of-plane components of the polarization, homogeneous and inhomogeneous tetragonal states, as well as peculiar laminar nanodomains.

DOI: 10.1103/PhysRevLett.93.196104

PACS numbers: 68.55.-a, 77.22.Ej, 77.80.Bh, 77.84.Dy

Ferroelectric thin films are of increasing technological interest because of the need in miniaturization of devices [1]. An intriguing problem in these films concerns their polarization patterns. For instance, the various following patterns have been recently predicted or observed: out-of-plane *monodomains* [2–5], 180° out-of-plane *stripe domains* [5,6], 90° multidomains that are oriented *parallel* to the film [7], and *microscopically paraelectric* phases [4]. The fact that dramatically different patterns have been reported for similar *mechanical* boundary conditions supports a concept discussed in Refs. [4,8], namely, that they arise from different *electrical* boundary conditions. More precisely, real thin films are likely neither in ideal open-circuit (OC) conditions, for which unscreened polarization-induced surface charges can generate a large depolarizing electric field along the growth direction [9], nor in ideal short-circuit (SC) conditions, which are associated with a vanishing internal field resulting from the full screening of surface charges, but rather experience a situation in between. The *amount* of surface charges' screening in thin films can vary from one experimental setup to another, possibly generating *different* polarization patterns [4,5].

Phenomenological and atomistic models have provided deep insight into thin films, but “only” for ideal OC or SC conditions (see Refs. [6,7,10], and references therein). First-principles calculations with electrical conditions falling between these two extremes have been performed, but the small used supercell size may have prevented the prediction of domains [4]. Finally, experimentally extracting the magnitude of the internal field is a challenging task. A precise correlation between the amount of screening of surface charges and the morphology of the polarization pattern, and how this correlation depends on mechanical boundary conditions, are thus still lacking nowadays despite their importance. *Atomic-scale* details of multidomains—and their formation mechanism—are also scarce in ferroelectric thin films. One may also wonder if some uncompensated depolarizing fields can yield ferroelectric phases that do *not* exist in the corre-

sponding bulk material. Candidates for these latter anomalies are films made of alloys with a composition lying near their morphotropic phase boundary (MPB), because of the easiness of rotating their polarization [11].

In this Letter, we develop a first-principles-based scheme to investigate the effects of uncompensated depolarizing fields on the properties of $\text{Pb}(\text{Zr}_{1-x}\text{Ti}_x)\text{O}_3$ (PZT) films near their MPB, for different mechanical boundary conditions. Answers to the problems summarized above are provided. We find a rich variety of ferroelectric phases, including unusual triclinic and monoclinic states. We also observe complex nanodomains and reveal their formation and atomic characteristics.

We model PZT thin films that (i) are grown along the [001] direction (to be chosen along the z axis), (ii) are “sandwiched” between nonpolar systems (mimicking, e.g., air, vacuum, electrodes, and/or nonferroelectric substrates), (iii) have Pb-O terminated surfaces, and (iv) have a 50% overall Ti composition. Such structures are modeled by large periodic supercells that are elongated along the z direction and that contain a few number of B layers to be denoted by m , with the atoms being randomly distributed inside each layer. Typically, we use $10 \times 10 \times 40$ periodic supercells with m around 5. The nonpolar regions outside the film are thus altogether $40 - m$ lattice constant thick along the growth direction, which allows well-converged results for the film properties [6]. The total energy of such supercells is used in Monte Carlo simulations, and is written as

$$E_{\text{Heff}}(\{\mathbf{u}_i\}, \{\mathbf{v}_i\}, \boldsymbol{\eta}, \{\sigma_i\}) = \sum_i \beta 2\pi \frac{Z^2}{a^3 \epsilon_\infty} \langle u_{j,z} \rangle_s u_{i,z}, \quad (1)$$

where E_{Heff} is the energy of the ferroelectric film *per se*. Its expression and first-principles-derived parameters are those given in Ref. [11] for bulk PZT. \mathbf{u}_i are the local soft modes in unit cells i of the PZT film whose components along the z axis are denoted as $u_{i,z}$. \mathbf{v}_i are inhomogeneous strain-related variables inside these films, while $\boldsymbol{\eta}$ is the homogeneous strain tensor. The form of $\boldsymbol{\eta}$ is relevant to stress-free (all the components of $\boldsymbol{\eta}$ fully relax) versus

epitaxially strained (001) films ($\eta_6 = 0$ and $\eta_1 = \eta_2 = \delta$, with δ being the strain resulting from the lattice mismatch between PZT and the substrate, while the other components relax during the simulations [7,10]). $\{\sigma_i\}$ characterizes the atomic configuration [11]. The local modes and the inhomogeneous strain-related variables are forced to vanish outside the PZT films. Therefore, a depolarizing field implicitly occurs inside the film if this film has a component of its polarization along the growth direction. The second term of Eq. (1) mimics the effects of an *internal* electric field—that arises from the *partial or full screening* of polarization-induced charges at the *surfaces*—on the films properties. This energetic term is dependent on the Z Born effective charge, the a lattice constant, the ϵ_∞ dielectric constant of $\text{Pb}(\text{Zr}_{0.5}\text{Ti}_{0.5})\text{O}_3$, and the average of the z component of the local modes centered at the surfaces (denoted by $\langle u_{j,z} \rangle_s$, which is self-consistently updated during the simulations) [12]. This second term is also directly proportional to a β parameter that characterizes the *strength* of the E_d total electric field inside the film. Specifically, $\beta = 0$ corresponds to ideal OC conditions for which E_d has its maximum magnitude, while an increase in β lowers this magnitude. The value of β resulting in a vanishing total internal electric field is dependent on the supercell geometry [9]. This *short-circuit* β is denoted as β_{SC} in the following. It is found to be 0.69, for stress-free films associated with $m = 7$ and a supercell periodicity of 40 lattice constant along the z axis, by fitting the $T = 10$ K predictions delivered by Eq. (1) to a single result of Ref. [3]; that is, the polarization in the film layer that is farther away from the surfaces is along the z axis and has a magnitude equal to the one in the bulk [13]. Our resulting $T = 10$ K predictions for stress-free ultrathin films that are under SC electrical boundary conditions are remarkably similar to those of Ref. [3]. For instance, the polarization at the surfaces is significantly enhanced with respect to the bulk, and increases as the film thickness decreases. Reference [3] and our proposed scheme both predict that the layers exhibiting the smallest polarization are those next to the surface layers, and that the layer that is farther away from the surfaces has a larger polarization for $m = 5$ than for $m = 3$ or 7 (thus exhibiting a non-monotonic behavior versus thickness).

Having demonstrated that our approach can capture subtle details, we now apply it to study the effects of *uncompensated* depolarizing fields on the ground state of $\text{Pb}(\text{Zr}_{0.5}\text{Ti}_{0.5})\text{O}_3$ ultrathin films. The thickness is kept fixed at $m = 5$, while different mechanical conditions are adopted: (i) stress-free [Fig. 1(a)], (ii) a tensile strain $\delta = +2.65\%$ [Fig. 1(b)], and (iii) a compressive strain $\delta = -2.65\%$ [Fig. 1(c)]. More precisely, Fig. 1 shows the predicted (absolute value of the) Cartesian components $\langle u_x \rangle$, $\langle u_y \rangle$, and $\langle u_z \rangle$ along the [100], [010], and [001] directions, respectively, of the average of the local-mode vectors in the film, as a function of β/β_{SC} and at

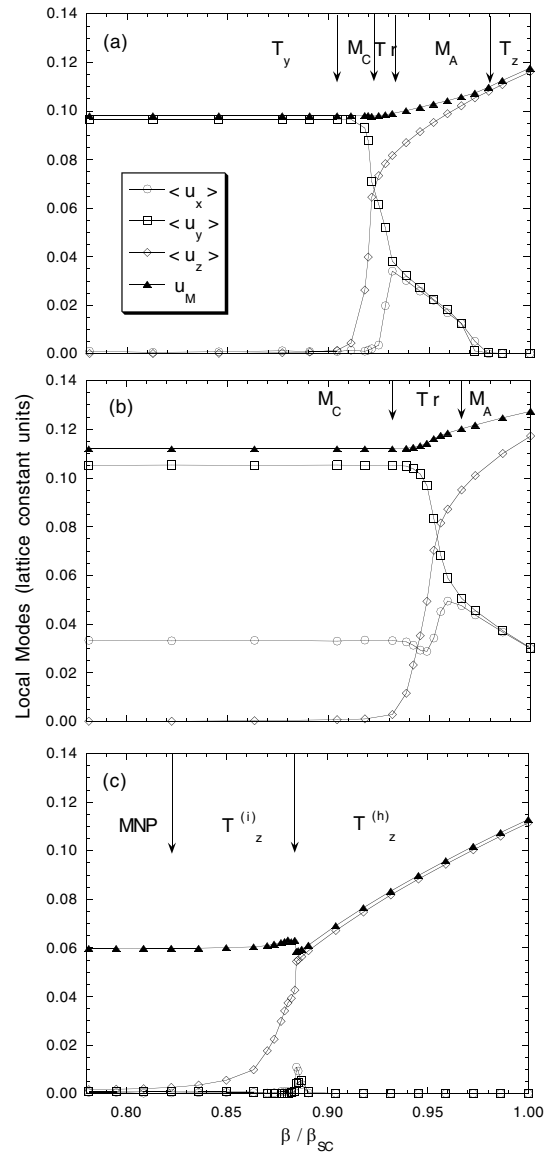


FIG. 1. Cartesian components of the film average of the local-mode vectors, as a function of the β/β_{SC} parameter in (001) $\text{Pb}(\text{Zr}_{0.5}\text{Ti}_{0.5})\text{O}_3$ ultrathin films having a $m = 5$ thickness, at $T = 10$ K. Panel (a) displays the predictions for stress-free films. Panels (b) and (c) show the results for a tensile and compressive strain of 2.65%, respectively. The arrows indicate the values of β/β_{SC} around which phase transitions occur. (Note that an orthorhombic phase also occurs for the stress-free film, for a single value of β/β_{SC} located at the M_C -to-Tr junction.) The results for β/β_{SC} down to zero are not shown since they are identical to those associated with the lowest values of β/β_{SC} displayed here. $10 \times 10 \times 40$ supercells are used.

$T = 10$ K. Figure 1 also displays the behavior of u_M , which is defined as $u_M = \sqrt{\langle u_x^2 + u_y^2 + u_z^2 \rangle}$ and thus provides a measure of the *local* polarizations.

Under *stress-free* conditions, the film has a polarization aligned along the z axis for (large) values of β that correspond to a screening of at least 98% of the

polarization-induced surface charges. This results in a tetragonal state to be denoted by T_z . On the other hand, when β becomes smaller than $\approx 0.904\beta_{SC}$, the internal field along the growth direction would be too strong to allow an out-of-plane component of the local mode [6]. As a result, the polarization aligns along an *in-plane* $\langle 010 \rangle$ direction. The corresponding ferroelectric phase is denoted as T_y . The most striking result for stress-free PZT films is the polarization path when going from T_z to T_y . As β/β_{SC} decreases from 98% to 90.4%, the polarization continuously rotates and passes through *three low-symmetry* phases: a so-called monoclinic M_A state [14] occurring for $0.932 \leq \beta/\beta_{SC} \leq 0.98$, and for which $\langle u_y \rangle$ and $\langle u_x \rangle$ are nonzero, equal to each other and smaller than $\langle u_z \rangle$; a triclinic Tr phase, for β/β_{SC} ranging between 92.2% and 93.2%, that is characterized by a local mode with nonzero and different Cartesian components; and a so-called monoclinic M_C ground state [14], when β/β_{SC} ranges between 90.4% and 92.2%, for which $\langle u_x \rangle$ vanishes while $\langle u_y \rangle$ becomes larger than $\langle u_z \rangle$. Interestingly, neither the Tr nor the M_C state is the ground state of PZT bulks. On the other hand, both phases exist for PZT bulks under external electric fields [15], which is consistent with the fact that the unusual Tr and M_C phases of Fig. 1(a) are induced by the depolarizing fields in the film. Moreover, all the low-symmetry states of Fig. 1(a) are stable only for compositions lying near the MPB of bulk PZT since we found that the M_A , Tr, and M_C phases disappear in favor of T_z for higher Ti concentration.

Comparing Fig. 1(b) with Fig. 1(a) reveals that films under a *tensile* strain react to depolarizing fields in a different way. In particular, both the end-member phases (T_z and T_y) of Fig. 1(a) disappear. The reason for the vanishing of T_z is that tensile strains favor in-plane components of the local modes because of the well-known coupling between strain and polarization. Consequently, T_z transforms into a M_A phase for large-enough δ strains. These epitaxial constraints—and more precisely the fact that η_2 cannot be different than η_1 —generate an in-plane component of the polarization along the $[100]$ direction in addition to a larger component along the $[010]$ direction, for small β . T_y thus becomes a M_C phase when going from stress-free to tensile conditions [16].

Conversely, a large-enough *compressive* strain annihilates the (in-plane) $\langle u_x \rangle$ and $\langle u_y \rangle$ components of the local mode for *any* β [see Fig. 1(c)]. Two macroscopically different phases result from this annihilation: a macroscopically nonpolar phase (MNP) for β smaller than $0.822\beta_{SC}$ and a ferroelectric tetragonal T_z phase for larger β . T_z can be further separated into two microscopically different phases. For $\beta/\beta_{SC} \geq 0.884$, the local polarizations all point along the growth direction and have similar magnitude, since $\langle u_z \rangle$ is nearly equal to u_M . The resulting state is referred to as $T_z^{(h)}$. On the other hand, when β ranges between 82.2% and 88.4% of β_{SC} , $\langle u_z \rangle$

becomes smaller than u_M . This characterizes a locally inhomogeneous polar state to be denoted by $T_z^{(i)}$. Another striking feature that can be extracted from Fig. 1(c) when looking at $\langle u_z \rangle$ and u_M is that the MNP phase has a relatively large magnitude for its local polarizations. To provide a detailed *microscopic* insight of compressively strained thin films, Figs. 2(a)–2(c) display a snapshot of (very large) $24 \times 24 \times 40$ supercell simulations yielding a $T_z^{(h)}$, $T_z^{(i)}$, and MNP phase, respectively. Figure 2(a) confirms that $T_z^{(h)}$ is locally homogenous. $T_z^{(i)}$ is likely the phase observed in Ref. [2] since this phase also occurs

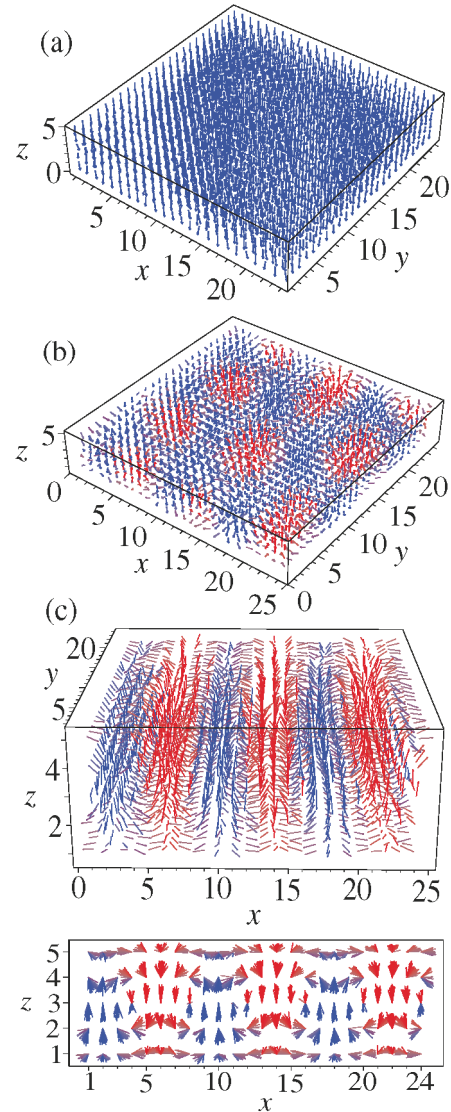


FIG. 2 (color). Three-dimensional polarization patterns in (001) $\text{Pb}(\text{Zr}_{0.5}\text{Ti}_{0.5})\text{O}_3$ films having a $m = 5$ thickness and under a compressive strain of -2.65% , at $T = 10$ K. Panels (a), (b), and (c) correspond to a β/β_{SC} parameter of 94.5% ($T_z^{(h)}$ phase), 87.7% ($T_z^{(i)}$ phase), and 80.8% (MNP phase), respectively. The bottom of (c) shows the projection of the 3D picture into an xz plane. Red (blue) indicates local dipoles having a positive (negative) component along the z axis. $24 \times 24 \times 40$ supercells are used.

for compressive strain and large screening of the surface charges. More striking, Fig. 2(b) reveals that $T_z^{(i)}$ is characterized by the formation of *nanodomains* having local dipoles that are aligned in an opposite direction with respect to the macroscopic polarization. These “bubble” nanodomains propagate throughout the entire thickness of the film but are *laterally* confined. $T_z^{(i)}$ is likely the phase experimentally seen in Ref. [5], and denoted there as F_γ , since this phase exhibits features that are consistent with our inhomogeneous $T_z^{(i)}$, namely, (i) compressive strain conditions and partially compensated depolarizing fields, (ii) a nonzero spontaneous polarization along the z axis, and (iii) broad diffraction peaks. In the MNP state [see Fig. 2(c)], the nanodomains have laterally “percolated,” resulting in the formation of nanoscale 180° (out-of-plane) stripe domains. Such peculiar multidomains are consistent with the F_α and F_β phases observed in Ref. [5] and with the antiparallel dipole configurations of Refs. [6,7]. Another interesting feature revealed by Fig. 2(c) is that the morphology of these nanodomains contrasts with the two “simplest” pictures of out-of-plane 180° domains found in magnetic films, namely, the flux-closure domain structures and the open-stripe structures [17]. In particular, each nanodomain of Fig. 2(c) that is terminated at one surface by significant in-plane and relatively small out-of-plane polarizations (to decrease the depolarizing field) has a neighboring nanodomain that is terminated at this surface by rather large out-of-plane polarizations (as driven by the large compressive strain). The junction between these two domains occurs via a rotation of the polarization (to minimize the energetical cost related to the polarization gradient, and to close the dipole flux). These complex nanodomains thus result from a subtle competition between different interactions, as similar to the fact that the balance between demagnetization, strain, exchange, and/or magnetic anisotropy can yield very complicated phase behavior in magnetic ultrathin films [18]. More specifically, the laminar nanodomains of Fig. 2(c) exist only for compressive strain and a large-enough depolarizing field, as consistent with the experimental conditions of Ref. [5] and the theoretical findings of Refs. [6,7]. Finally, Fig. 2(c) also shows that the predicted period Λ of the laminar domains is $\approx 8a_{\text{in}}$, where a_{in} is the in-plane lattice constant. This remarkably agrees with the measurements of Ref. [5] yielding $\Lambda = 37 \text{ \AA}$ for 20 \AA -thick PbTiO_3 films. [Other calculations we performed, using $n \times n \times 40$ supercells with $n = 16, 18, 20,$ and 24 , confirm that Λ ranges between $8a_{\text{in}}$ and $9a_{\text{in}}$, as well as the peculiar domain morphology of Fig. 2(c).]

We thank D. D. Fong, R. Haumont, J. Junquera, I. Naumov, S. K. Streiffer, and C. Thomson for useful dis-

cussions. This work is supported by ONR Grants No. N 00014-01-1-0365 and No. 00014-01-1-0600 and NSF Grant No. DMR-9983678.

-
- [1] *Ferroelectric Memories*, edited by J. F. Scott (Springer-Verlag, Berlin, 2000).
 - [2] T. Tybell, C. H. Ahn, and J.-M. Triscone, *Appl. Phys. Lett.* **75**, 856 (1999).
 - [3] P. Ghosez and K. M. Rabe, *Appl. Phys. Lett.* **76**, 2767 (2000).
 - [4] J. Junquera and P. Ghosez, *Nature (London)* **422**, 506 (2003).
 - [5] S. K. Streiffer *et al.*, *Phys. Rev. Lett.* **89**, 067601 (2002).
 - [6] S. Tinte and M. G. Stachiotti, *Phys. Rev. B* **64**, 235403 (2001).
 - [7] Y. L. Li *et al.*, *Appl. Phys. Lett.* **81**, 427 (2002).
 - [8] J. Junquera *et al.*, *Abstract of Fundamental Physics of Ferroelectrics, Colonial Williamsburg, VA, 2004* (NISTIR, Gaithersburg, 2004), Abstract No. NISTIR 7106, p. 86.
 - [9] B. Meyer and D. Vanderbilt, *Phys. Rev. B* **63**, 205426 (2001).
 - [10] N. A. Perstev *et al.*, *Phys. Rev. B* **67**, 054107 (2003).
 - [11] L. Bellaiche, A. García, and D. Vanderbilt, *Phys. Rev. Lett.* **84**, 5427 (2000); *Ferroelectrics* **266**, 41 (2002).
 - [12] Decomposing the total energy of thin film under uncompensated fields as a sum of one term depending on bulk parameters and a second term associated with internal field, as we do in Eq. (1), has been proposed in Refs. [4,8] and reproduces well direct first-principles *macroscopic* results [4]. Our present scheme can also capture detailed *atomic* features because, unlike Refs. [4,8], (i) finite size effects are included in both energetic terms of Eq. (1), and (ii) our depolarizing field depends on polarization at the surface. Surface or interface effects going beyond the generation of surface charges (e.g., interface bonding) are not included here, because such effects should play a much lesser role than the residual depolarizing field on the film properties [4].
 - [13] β_{SC} is $+0.774$ and $+0.732$ for $m = 3$ and 5 , when using $n \times n \times 40$ supercells.
 - [14] D. Vanderbilt and M. H. Cohen, *Phys. Rev. B* **63**, 094108 (2001).
 - [15] L. Bellaiche, A. García, and D. Vanderbilt, *Phys. Rev. B* **64**, 060103(R) (2001).
 - [16] The disappearance of the T_z and the T_y phases under tensile conditions is a MPB feature, since it does not occur in PZT ultrathin films having higher Ti composition, as consistent with Ref. [10].
 - [17] L. D. Landau and E. M. Lifschitz, *Electrodynamics of Continuous Media* (Pergamon Press, New York, 1984).
 - [18] O. Portmann, A. Vaterlaus, and D. Pescia, *Nature (London)* **422**, 701 (2004).